

# Design and Fabrication of a Two-Dimensional Superconducting Bolometer Array for SAFIRE

Dominic J. Benford<sup>† a</sup>, George M. Voellmer<sup>a</sup>, James A. Chervenak<sup>a</sup>,  
Kent D. Irwin<sup>b</sup>, S. Harvey Moseley<sup>a</sup>, Rick A. Shafer<sup>a</sup>, Johannes G. Staguhn<sup>a,c</sup>

*a* NASA / Goddard Space Flight Center *b* NIST – Boulder *c* SSAI

## ABSTRACT

The Submillimeter and Far-InfraRed Experiment (SAFIRE) on the SOFIA airborne observatory will employ a large-format, two-dimensional, close-packed bolometer array. SAFIRE is an imaging Fabry-Perot spectrometer operating at wavelengths between 100 $\mu$ m and 700 $\mu$ m. The array format is 16x32 pixels, using a 32-element multiplexer developed in part for this instrument. The low backgrounds achieved in spectroscopy require very sensitive detectors with NEPs of order 10<sup>-19</sup> W/ $\sqrt$ Hz. An architecture which permits 512 pixels to be placed adjacent to each other in an area the size of a postage stamp, integrate them with multiplexers, and provide all the necessary wiring interconnections is a complex proposition, but can be achieved. Superconducting detectors can be close-packed using the Pop-Up Detector (PUD) format, and SQUID multiplexers operating at the detector base temperature can be intimately coupled to them. The result is a compact array, easily scalable to kilopixel arrays. We describe the PUD architecture, superconducting transition edge sensor bolometers we have manufactured and tested using the PUD architecture, and the electronics of SQUID multiplexed readouts. We show the design and assembly of the mechanical model of a 512-element bolometer array.

**Keywords:** bolometer array, transition edge sensor, superconducting multiplexer, SQUID multiplexer, SOFIA

## 1. INTRODUCTION

The Submillimeter and Far-InfraRed Experiment (SAFIRE) on the SOFIA airborne observatory is designed to be a wide-field imaging spectrometer with moderate spectral resolving power<sup>1</sup>. It will achieve a resolution of about 300km/s, continuously tunable over the 145 $\mu$ m-655 $\mu$ m range. Combining the low background present at the high altitude of the observatory with the bandwidth narrowing yields a requirement for a detector as or more sensitive than any yet made at this wavelength. Additionally, the requirement for a wide field of view demands an array containing hundreds of pixels. The largest array of detectors for far-infrared wavelengths has been built for the HAWC and SHARC-II instruments<sup>2</sup>, each containing 384 semiconducting bolometers operating at ~200mK coupled to 384 JFET amplifiers operating at ~120K. The mechanical, thermal, and optical design of this array is a challenging engineering exercise.

Recent research had led to a new approach to building arrays of many bolometers. Instead of a semiconducting thermistor, a superconducting transition edge sensor (TES) is used to read out the detector temperature. A TES bolometer has a faster response time than an identically designed, same-sensitivity semiconducting bolometer (or a more sensitive bolometer for the same response time) due to the strong negative electrothermal feedback intrinsic in a voltage-biased TES<sup>3</sup>. TES bolometers are inherently low impedance devices, so they are well-matched to being read out by DC SQUID amplifiers<sup>4</sup>. These amplifiers have a large noise margin over the TES Johnson noise and bolometer phonon noise. This permits the bolometer to be read out in a multiplexed fashion by a suitable SQUID multiplexer<sup>5</sup>, potentially vastly reducing the amplifier size and the wire count. Because SQUID multiplexed amplifiers operate at the base temperature of the bolometer, they can be coupled very closely, removing the complex interfaces necessary with semiconducting bolometers. In light of these advantages, we have chosen to develop an array of multiplexed superconducting bolometers for SAFIRE. Herein, we describe the TES bolometers we have manufactured and tested, the electronics of SQUID multiplexed readouts, and the design and assembly of a 512-element bolometer array.

---

<sup>†</sup> Corresponding Author: Dominic J. Benford; [dominic.benford@gsfc.nasa.gov](mailto:dominic.benford@gsfc.nasa.gov); 301.286.8771; Code 685, NASA/GSFC, Greenbelt, MD 20771; [http://lasp-nts1.gsfc.nasa.gov/irbranch/Dominic\\_J\\_Benford.html](http://lasp-nts1.gsfc.nasa.gov/irbranch/Dominic_J_Benford.html)

## 2. DETECTOR ARRAY REQUIREMENTS

On SOFIA, a large field of view is available with diffraction-limited performance in the far-infrared. The spatial resolution at  $200\mu\text{m}$  is  $20''$ . It is therefore reasonable to set the plate scale in the focal plane to  $10''$  per pixel. In order to produce detectors with absorption efficiency at wavelengths of  $\sim 650\mu\text{m}$ , it is useful to set the pixel scale to  $1\text{mm}$ . The spectral resolving power is generated by a high-resolution Fabry-Perot with an order-sorting Fabry-Perot and filter wheel. A convenient beamwidth to propagate through the optical setup would be  $\sim 50\text{mm}$  in diameter, which, for a resolving power of  $300\text{km/s}$ , yields a maximum field of view of  $6'$  diameter. This field would contain about 1000 pixels of  $10''$  square, but in an inconvenient distribution on the focal plane. We have instead chosen to use a 32-element multiplexer that would couple to a linear detector array that is conveniently close to the field size. The maximum array format that fits within the  $6'$  diameter is then a  $16 \times 32$  array, assuming closely packed detectors.

The background power on SOFIA is largely determined by the emissivity of the atmosphere, shown in Figure 1. This can be translated into an atmospheric photon noise equivalent power (NEP), as shown in Figure 2. The SAFIRE detectors will need to achieve a phonon and Johnson noise sum of  $< 3 \cdot 10^{-18} \text{ W}/\sqrt{\text{Hz}}$  in order to be background-limited, and must be able to absorb up to  $\sim 0.3\text{pW}$  in order to avoid saturation. This puts a stiff requirement on the dynamic range of the bolometers, in that the ratio of maximum power detected to the minimum power detectable in unity bandwidth is about  $10^5$ .

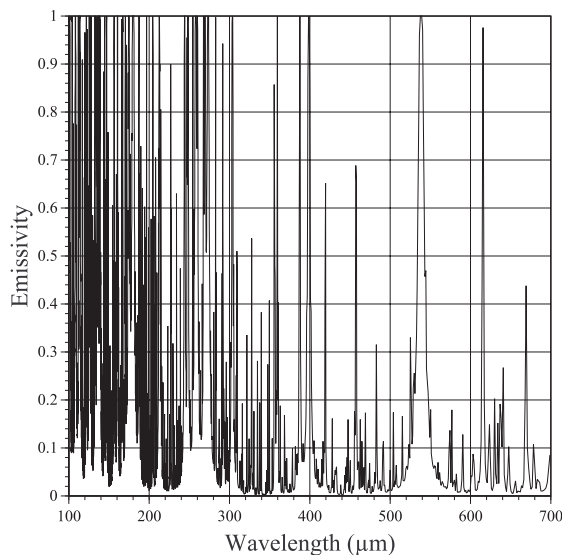


Figure 1. Atmospheric emission from SOFIA altitudes, assuming  $5\mu\text{m}$  precipitable water vapor<sup>6</sup>

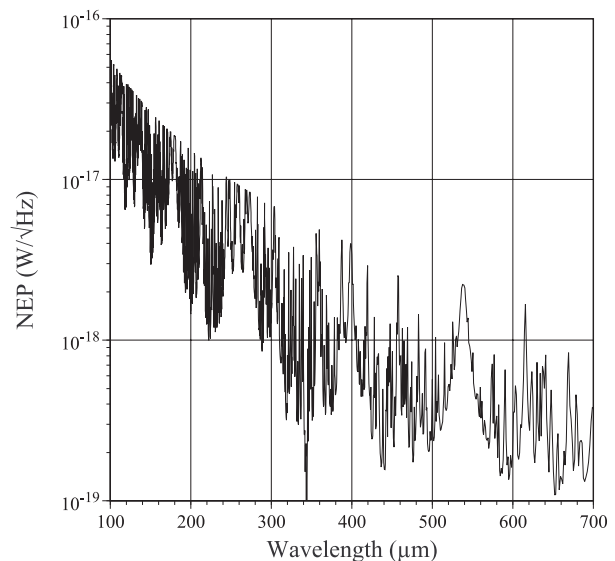


Figure 2. Photon noise equivalent power from the emission shown in Figure 1.

## 3. DESIGN OF CLOSE-PACKED ARRAY

Bolometers require very low thermal conductance supports in order to make them sensitive. These supports are usually long, thin wire-like structures that operate in tension and occupy appreciable focal plane area, often being larger in area than the optically active portion of the bolometer itself. Along with these supports, wiring is needed to connect to the bias and readout circuitry; this is often another space-consuming portion of an array. How, then, can a bolometer array be manufactured with a high filling factor of optically active surface? Substantial effort at NASA's Goddard Space Flight Center has gone into the development of a novel solution that brings the mechanical and electrical connections out behind the bolometer. A rectangular bolometer absorber is manufactured in a thin silicon or silicon nitride membrane with four legs projecting out of the sides (Figure 3). These legs are folded beneath the absorber, forming a table-like structure with the supports under flexural rather than tensile stress (Figure 4). This approach is referred to as a "Pop-Up Detector" or PUD, by analogy to the deployment of similar structures in children's books.

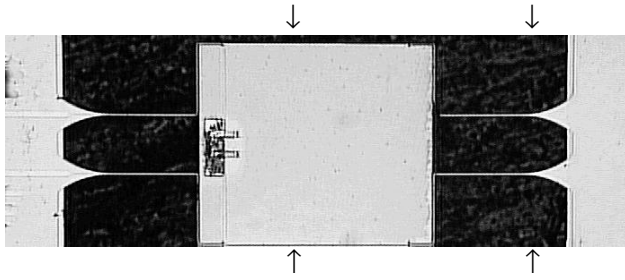


Figure 3. Single Pop-Up Detector; the arrows indicate the two fold lines, where a torsion bar hinge can be seen

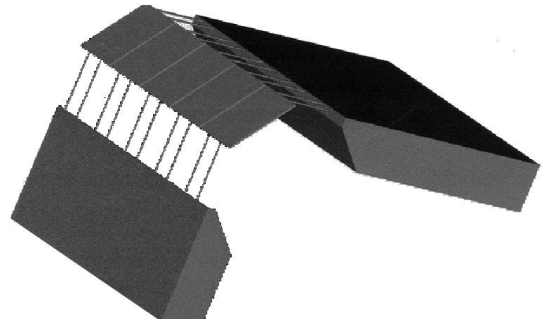


Figure 4. Illustration of the folding of a small linear array of Pop-Up Detectors.

The first large-scale PUD array has been built for the SHARC-II instrument on the Caltech Submillimeter Observatory and the HAWC instrument on SOFIA<sup>2</sup> (Figures 5 & 6). Both of these feature 12x32 bolometers using semiconducting thermistors, and will operate in broadband imaging cameras. These arrays have demonstrated the folding, stacking, and interconnection procedures necessary to make a close-packed array. Because of the much simpler thermal and mechanical interfacing possible with superconducting bolometers, we have redesigned the PUD assembly to produce an architecture that permits very compact, close-packed arrays of multiplexed bolometers.

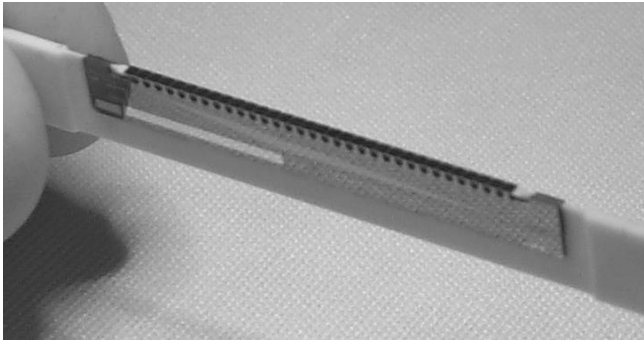


Figure 5. Photo of a folded 32-element array for the HAWC and SHARC-II instruments

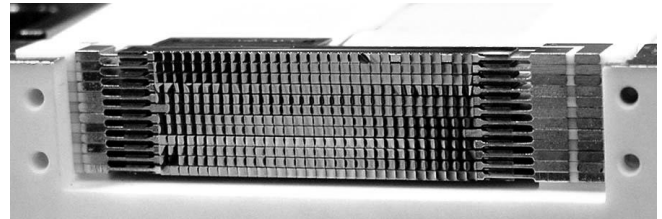


Figure 6. Photo of the assembled 12x32-element array for the SHARC-II instrument; the HAWC array will appear similar.

#### 4. INDIVIDUAL BOLOMETER DESIGN

A TES bolometer is fundamentally no different from a semiconducting bolometer, other than a change in the thermistor that has substantial implications. Infrared light is absorbed in the bolometer and converted into heat which warms the detector of heat capacity  $C$  above its nominal temperature  $T_{bias}$  (Figure 7). This temperature change is converted into a resistance change which is measured electrically. The heat is conducted away through a thermal conductance  $G$  to a heat sink at  $T_{bath}$ . A superconducting transition at temperature  $T_C$  yields an extremely sharp but continuous change in resistance from near zero to the normal state resistance (Figure 8). A unitless measure of the sharpness is defined as

$$\alpha \equiv \frac{d \log R}{d \log T} = \frac{T}{R} \frac{dR}{dT} \approx \frac{2T_C}{\Delta T}$$

where  $\alpha$  is called the sensitivity and  $\Delta T$  is the approximate transition width. The response time of a bolometer is typically the thermal time constant,  $\tau = C/G$ . However, TES bolometers can be faster by means of electrothermal feedback. When biased onto the transition, power is dissipated in the thermistor as  $P = V^2/R$ . When optical power is applied, the thermistor warms up, increasing its resistance dramatically. The bias power drops to compensate, bringing the TES back towards the stable bias point. The effective time constant is then approximately  $\tau_{eff} = \tau n / \alpha$ , where  $n$  is the temperature index of the thermal conductance. At low frequencies ( $(\omega \tau_{eff})^2 \ll 1$ ), the Johnson noise is suppressed through the action of the electrothermal feedback by a factor of  $(n/\alpha)^2$ . The end result of this is that the intrinsic noise of a TES bolometer is typically dominated by the phonon noise alone.

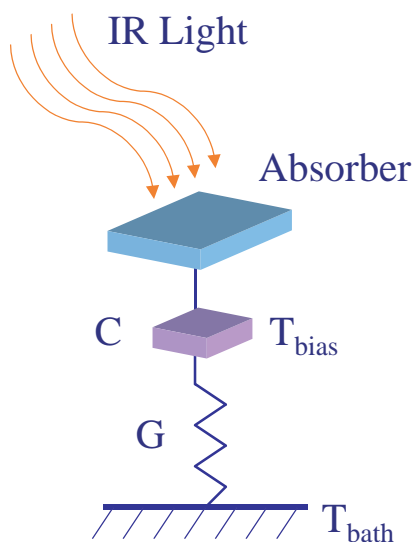


Figure 7. Simple thermal model of a bolometer.

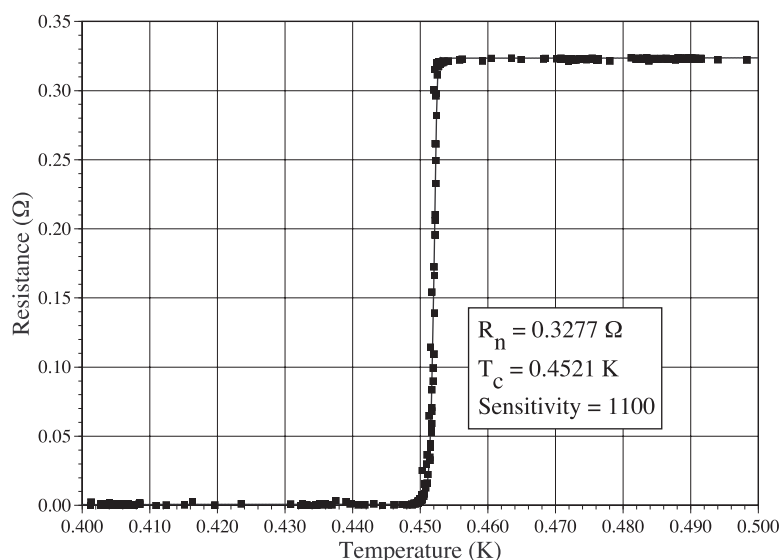


Figure 8. Resistance of a superconducting transition edge sensor as a function of temperature near the transition.

Superconducting transitions can be made in several ways. In order to produce a thermistor with a tunable  $T_C$  and with a known resistance, we manufacture superconducting-normal bilayers. The superconductor, in this case a thin film of molybdenum, has its transition temperature reduced by proximity to a thin film of a normal metal such as gold or copper. This process is described more fully by Chervenak et al.<sup>5</sup>. The thermistor is manufactured by deposition and photoetching to produce a small ( $50\mu\text{m} \times 100\mu\text{m} \times 0.1\mu\text{m}$ ) active volume.

The voltage-current characteristic of a TES bolometer is quite different from that of a semiconducting bolometer. If we consider a voltage-biased TES cooling down from the normal state, the device exhibits a constant resistance ( $I = V/R$ ) (Figure 9). If we lower the bias voltage, at some point the bias power becomes too little to keep the device in the normal state, and it will begin to drop in resistance. Because the transition width is small, the TES is nearly isothermal at any point on the transition, and so the total dissipated power must be constant. In this case, the current becomes a hyperbolic function of the voltage,  $I = P/V$ . At some point, the bias current reaches a maximum value (set by electronics) and the TES becomes superconducting. The responsivity of a TES on its transition is approximately  $1/V$  (A/W).

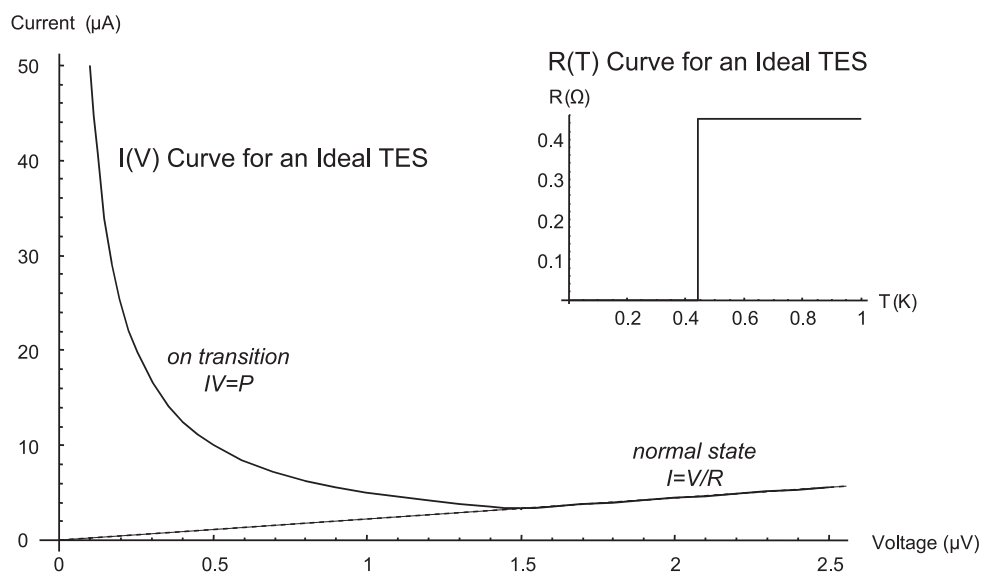


Figure 9. Voltage-current characteristic of an ideal superconducting transition edge sensor.

## 5. 32-ELEMENT LINEAR ARRAY DESIGN

When designing an array using the PUD architecture, the unit cell is one of the first choices to make. We have chosen to use linear arrays of 32 detectors, primarily due to the fact that present technology makes possible a 32-input SQUID multiplexer, built at NIST-Boulder. For early prototype purposes, we have manufactured 8-element linear arrays of  $1\text{mm}^2$  pixels (Figure 10) featuring appropriate thermal conductances for use in SAFIRE, although the transition temperature was set to 440mK for convenience of testing with a  $^3\text{He}$  refrigerator<sup>7</sup>. SAFIRE's adiabatic demagnetization refrigerator provides a 100mK base temperature.

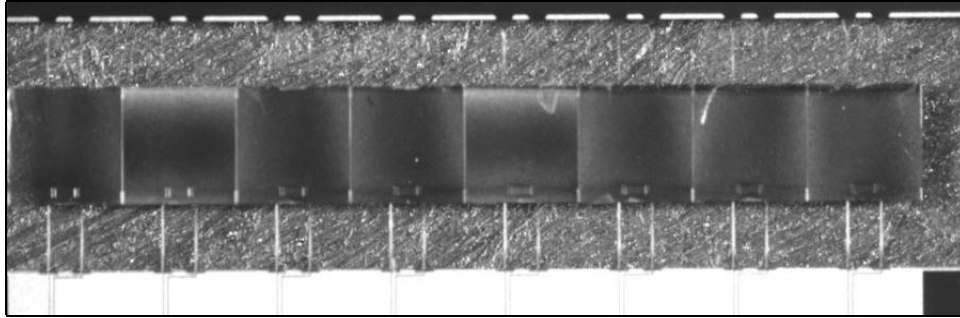


Figure 10. Photo of an eight-element linear array of superconducting bolometers. Each pixel is  $1\text{mm}$  on a side and is suspended by four legs to allow folding. The superconducting bilayer is the rectangle near the bottom edge of each pixel.

The 32-element PUD array for SAFIRE is designed as an extension of the 8-element array, as shown in Figure 11. New features include alignment holes and wiring with on-chip bias resistors. Because these resistors are low value – typically a few  $\text{m}\Omega$  – it is useful to use photolithography to yield the resistance precision necessary in a small size. The bond pads are arranged so that each detector has a bias shunt resistor, but ganged together in series to deliver the same bias to all detectors (Figure 12). When the 32-element detector array is folded, the alignment holes permit several of them to be stacked together on dowel pins to produce a single two-dimensional array.

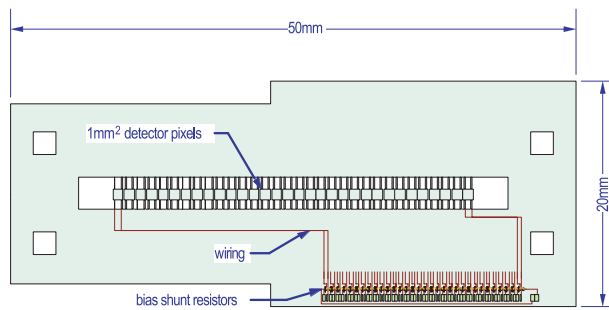


Figure 11. Layout of a 32-element array with on-chip bias circuitry and assembly alignment holes.

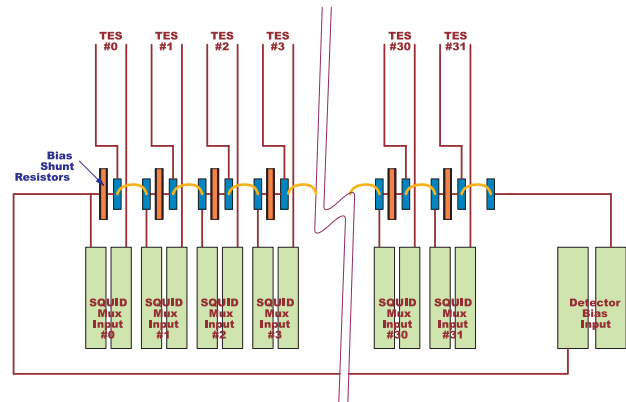


Figure 12. Layout of bond pads on the detector chip, showing circuitry for the bias shunt resistors.

## 6. 32-ELEMENT SQUID READOUT

A crucial element in the design of a large-format array is the multiplexer. As a collaborative effort between NASA-Goddard and NIST-Boulder we have, over the past few years, made substantial progress in the use of SQUID multiplexers for the readout of low-impedance devices. An eight-input SQUID multiplexer/amplifier<sup>5</sup> has been used to demonstrate Johnson-noise-limited readout<sup>8</sup>, detection of infrared light with TES bolometers<sup>9</sup>, and operation in an astronomical application<sup>10</sup>. There is now a 32-input SQUID multiplexer with a more advanced architecture<sup>11</sup>, shown below in Figure 13. This multiplexer operates using time-domain multiplexing, and can operate at rapid switching rates with low channel-to-channel crosstalk. A second stage SQUID amplifier is included on this chip to provide sufficient output to drive the multiplexed signal to a SQUID amplifier located elsewhere.

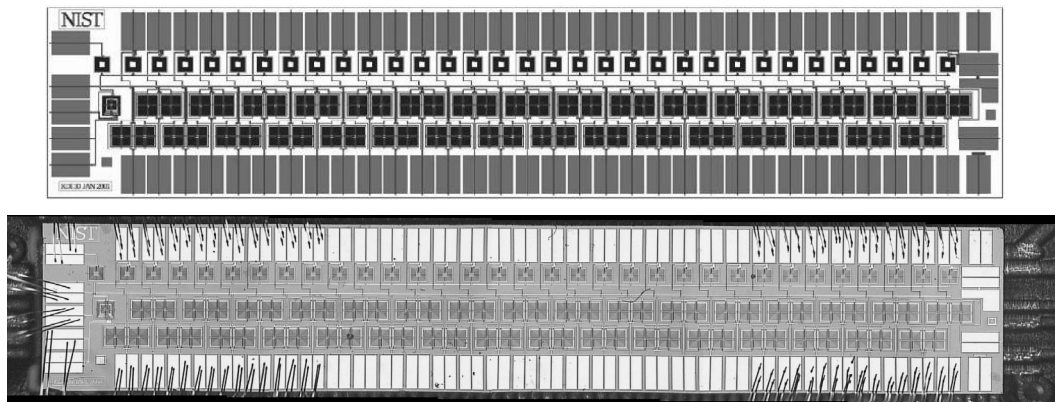


Figure 13. 32-input SQUID multiplexer chip manufactured at NIST-Boulder. (Top) design; (Bottom) photo.

The function of a SQUID readout is more complex than for a FET, due to the fact that the SQUID output is a periodic rather than linear function of the input. A SQUID transduces a measurement of magnetic flux into a voltage with extreme sensitivity. We use a voltage-biased TES sensor, so that the current varies as the resistance changes. This current is coupled to the SQUID through an inductor (Figure 14). The SQUID produces a voltage that is periodic in the input current. If we place a second inductor, called the feedback coil, next to the SQUID, we can introduce a current exactly opposite the measured current in the input coil. As the input coil current changes (as the TES resistance changes), the SQUID reads a differential current. The feedback current can be changed based on this difference to result in a nulled flux through the SQUID. The SQUID output is now a linear function of the input, and the feedback current is always equal to the current through the TES.

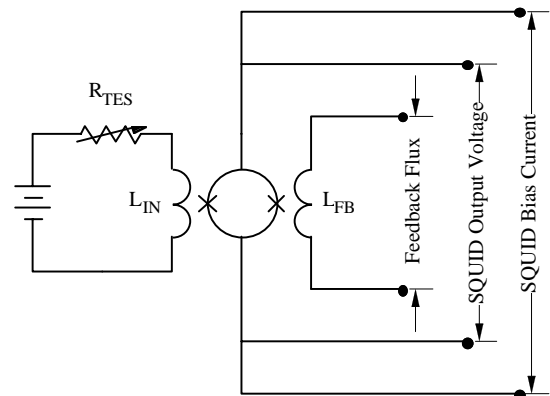


Figure 14. Simplified linearized SQUID amplifier reading a voltage-biased TES thermistor.

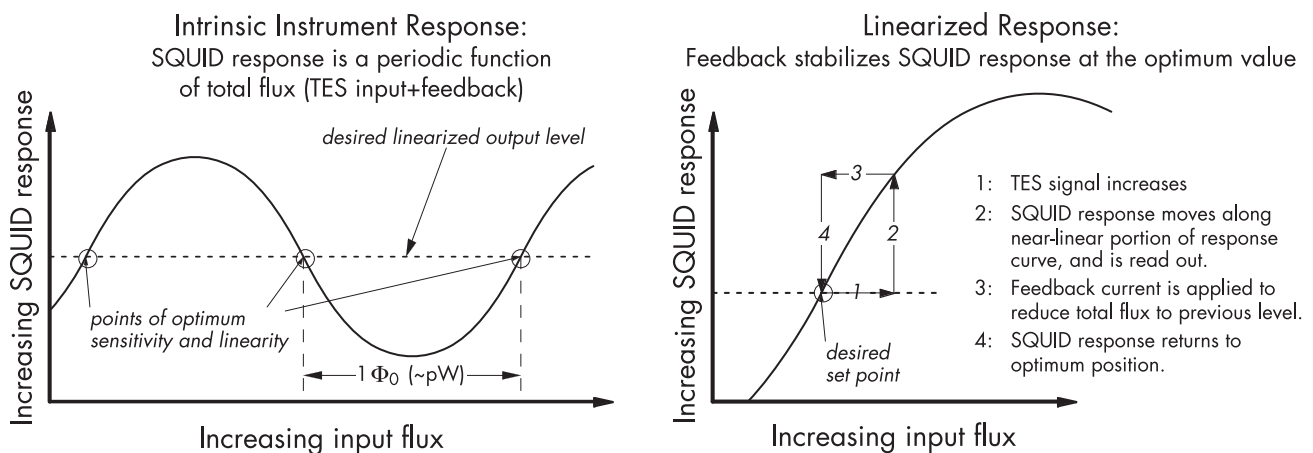


Figure 15. (Left) Approximate representation of the response of a SQUID multiplexed readout to a linearly increasing input signal. (Right) Illustration of the feedback method used to linearize the SQUID readout for multiplexed detectors.

In the case of a multiplexed SQUID readout, since several inputs are read through one output, the feedback process is somewhat more complicated, and is shown graphically in Figure 15. Under control by a computer, a given input SQUID is turned on and its differential current (the signal minus the feedback) is read out. This difference current is then nulled



by changing the feedback current, and its value – equal and opposite to the TES current – is stored for the future. The next SQUID is read out similarly, until all inputs have been read. On the next cycle, the previous readout of the TES current is looked up from memory, and its current is nulled with the previous feedback value. The SQUID then reads out the difference between the previous reading and the present reading, providing a linearized response.

A single column of the 16x32 SAFIRE detector array can be represented simply as a 32-element TES coupled to a 32-input SQUID multiplexer, as shown in Figure 16. To be complete, a 32-element integrating inductor needs to be included. The purpose of this inductor is to provide a bandpass filter on the TES circuit, which serves to integrate the TES signal. This results in the multiplexer being used to sample an already integrated signal, rather than merely integrating 1/32 of the time per channel. For noise purposes, the sampling time of the SQUID is smaller than that of the

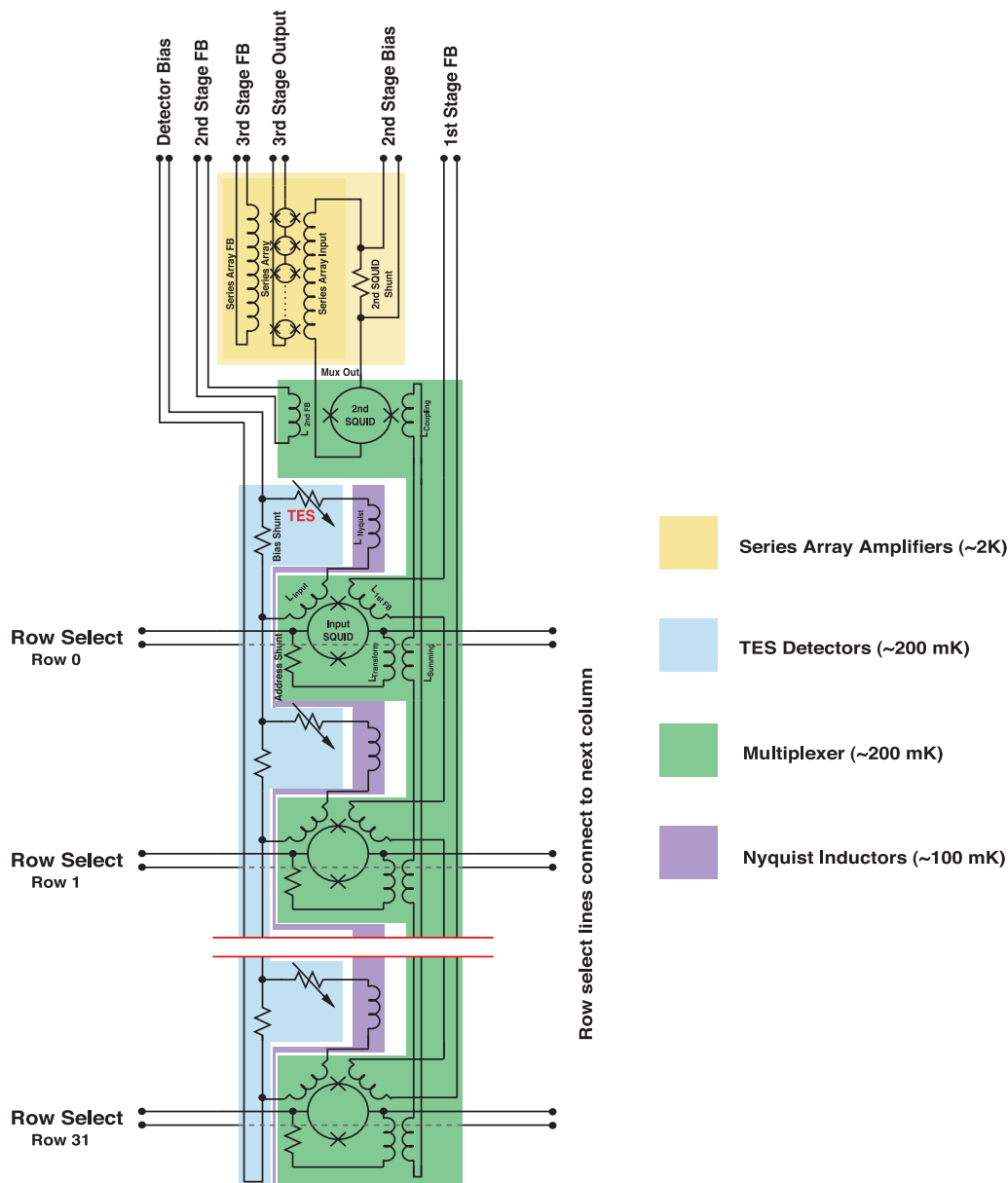


Figure 16. Schematic of a 32-element readout circuit comprised of a 32-element TES bolometer array coupled to a 32-element SQUID multiplexer with a 32-element integrating inductor and amplified by a 100-element SQUID amplifier.

TES, so the SQUID noise must be smaller (by a factor of at least  $1/\sqrt{32}$ ) than the noise of the input. The output of the multiplexer is amplified by a 100-element SQUID array, which boosts the signal up to a level easily handled by room temperature electronics. In order to add another column, lines to connect to the left and right are shown for carrying the signals that turn on the input SQUIDs.

The electronics for the SAFIRE bolometer array readout have been developed in a modular fashion, where the fundamental unit of array size is considered to be  $8 \times 32$ . SAFIRE therefore uses two sets of electronics, although several components (such as the addressing electronics) do not need to be duplicated. A block diagram for the electronics is shown in Figure 17. The warm electronics fit into two compact racks that mount to the SAFIRE cryostat and communicate with a data acquisition computer via fiber optic. The software for controlling the SAFIRE instrument and acquiring detector data is a generic Java-based environment called Instrument Remote Control (IRC)<sup>12</sup>.

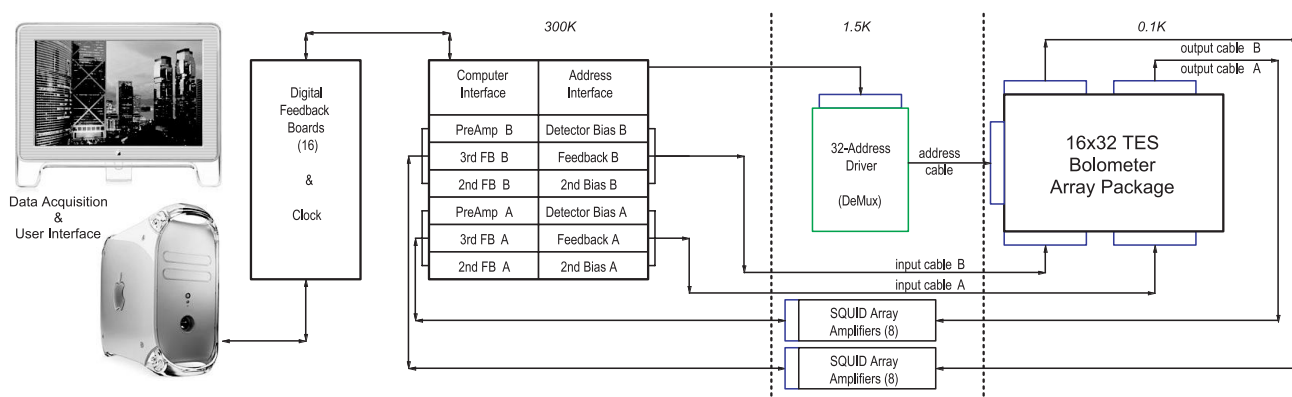


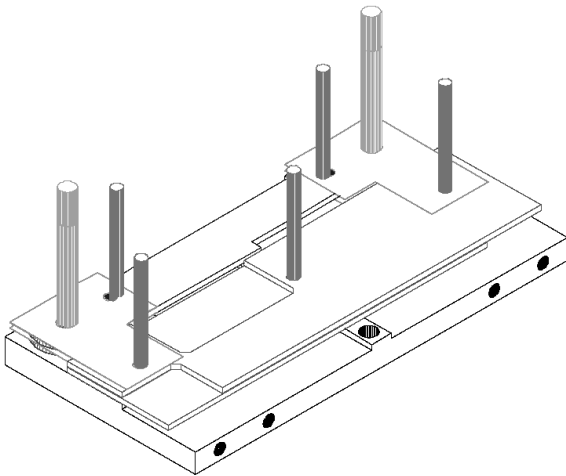
Figure 17. Block diagram for the SAFIRE 16x32 bolometer array electronics.

## 7. TWO-DIMENSIONAL ARRAY ASSEMBLY

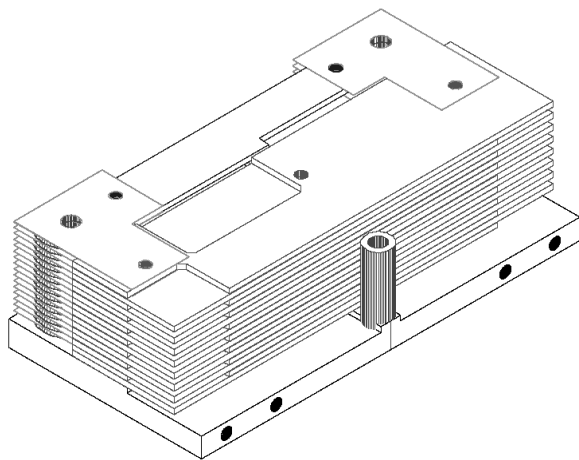
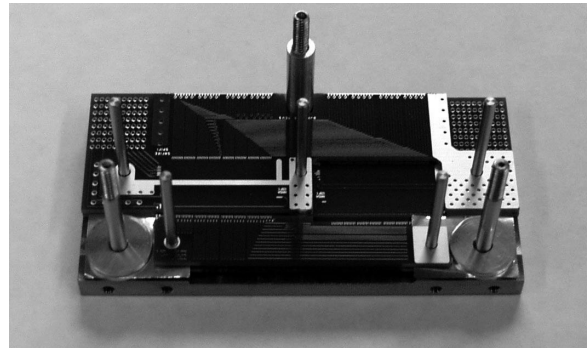
The assembly of a superconducting PUD array is designed to require very little difficult craftsmanship, provided that the individual detectors and SQUID multiplexers have been previously characterized and prepared. A folded PUD array and a circuit board carrying the SQUID multiplexer and Nyquist inductor is first installed on a baseplate, using alignment dowel pins to position them correctly. Wirebonds are used to connect the detector to the readout. The circuit board fans out to a set of holes into which cables are soldered, providing the attachments for all the electrical connections except the input SQUID addressing connections. This is shown in the top panels of Figure 18. A second PUD array and circuit board is then added atop the first, but this set is mirror-imaged such that the bond pad areas do not lie near each other. This permits space for wirebonds without the fear that subsequent stacked layers will crush the fragile interconnections. The process continues until all 16 of the PUD arrays and circuit boards are installed (middle panels of Figure 18). At this point, cabling for all the readouts would be dangling to the sides.

To complete the array fabrication, a circuit board to carry the input SQUID addressing connections is attached to the top, and wirebonds connect along the edges of all the circuit boards. This address bus ensures that all columns turn on their input SQUIDs simultaneously with the minimum number of wires. A top plate similar to the baseplate is bolted onto the stack of circuit boards, putting them into compression using springs (bottom panels of Figure 18). In this way, thermal contraction is accommodated. The top plate and baseplate are made of titanium, which has a coefficient of thermal expansion similar to that of the silicon PUD array. The titanium will also be superconducting at the operating temperature, so that Johnson noise from the metal structure does not couple into the SQUID multiplexers. A tower of stacked copper washers and foils provides thermal contact to each PUD array and circuit board. Finally, the cabling is bolted onto the end plates and mounting stanchions are attached. The PUD array is mounted by means of a thermally isolating kinematic Kevlar suspension<sup>13</sup> (Figure 19).

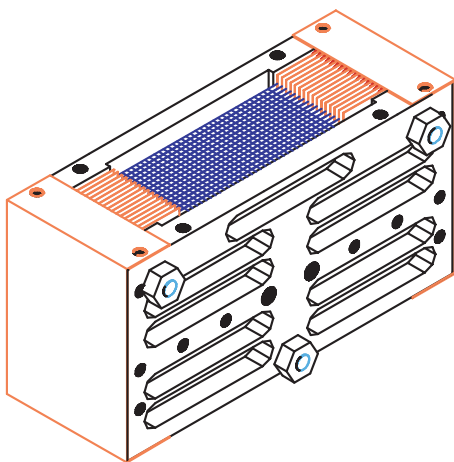
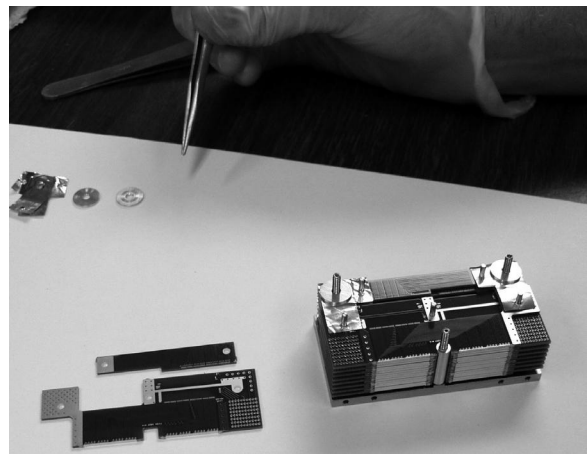




First two columns stacked:



All 16 columns stacked:



Array package completed:

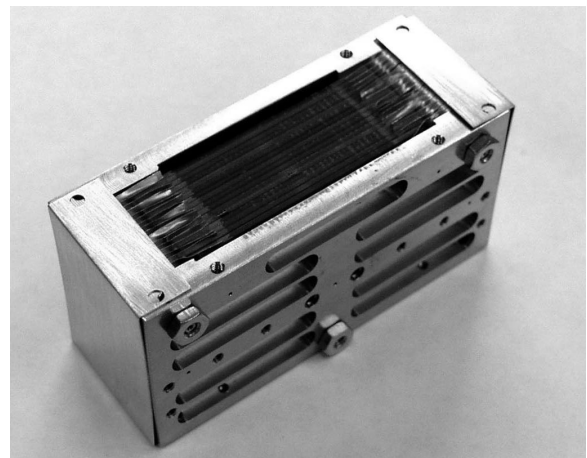


Figure 18. Stages in the assembly of the SAFIRE 16x32 bolometer array. The assembly pictured above is a mechanical prototype; the complete array will also have wires soldered to the circuit boards to make electrical connections, which are brought of the light-tight package through baffles to connectors mounted on the rear.

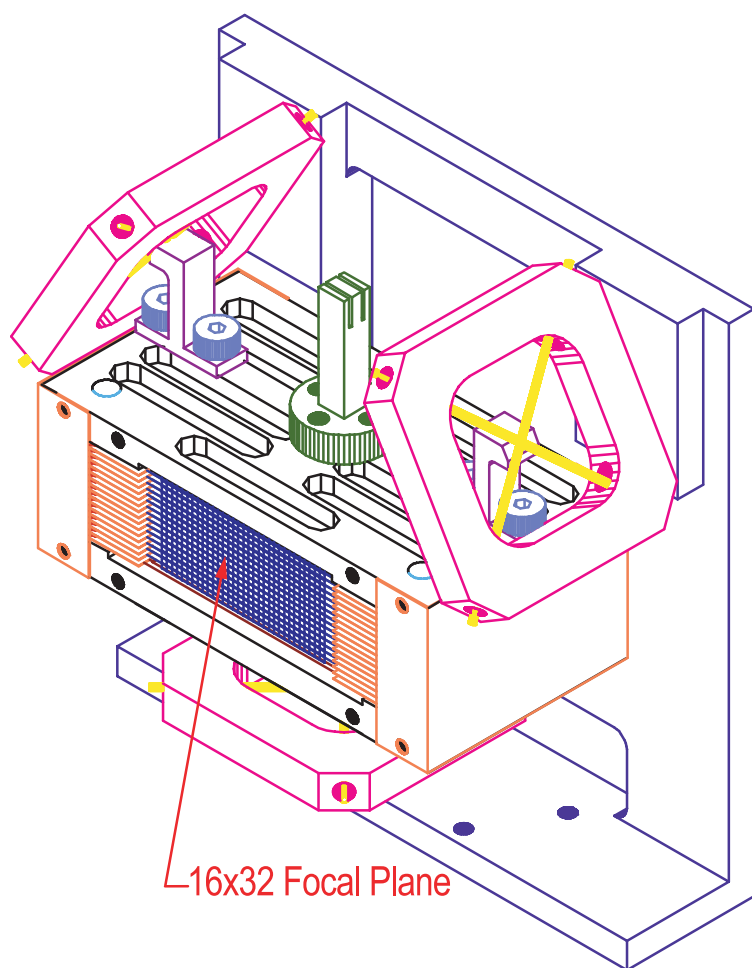


Figure 19. Completed detector array package, including mechanical and thermal attachments but with the electrical connectors not shown. The cold detector package is mounted by a mechanically stiff yet thermally isolating support, using a kinematic Kevlar suspension. The stub in the center of the detector package is the thermal attachment point.

## 8. SUMMARY

We have designed a 16x32 array of superconducting TES bolometers with integrated SQUID multiplexers for the SAFIRE instrument on SOFIA. Prototype detectors have been manufactured and tested in a 300mK setup. The electrical circuit has been designed with the goal of making a compact, low power multiplexed readout that can be intimately coupled with the detectors. An architecture for the assembly of the detectors using the PUD geometry to produce a compact, close-packed focal plane array has been illustrated. The fundamental unit for this approach is an 8x32 unit cell, which would provide a usable grating spectrometer array for instruments such as ZEUS<sup>14</sup>. A 16x32 array is being produced for the SAFIRE instrument and for the SPIFI instrument. Future instruments can use a 32x32 array using the same components, so that this design is compatible with kilopixel arrays.

## REFERENCES

1. Shafer, R.A., Moseley, S.H., Benford, D.J., Irwin, K.D., Pajot, F., Staguhn, J.G., & Stacey, G.J. 2002, these proceedings; "*Far-Infrared Imaging Spectroscopy with SAFIRE on SOFIA*"
2. Dowell, C.D. et al. 2002, these proceedings; "*SHARC II: A Caltech Submillimeter Observatory Facility Camera with 384 Pixels*"; Harper, D.A. et al. 2000, Proc. SPIE #4014, "Airborne Telescope Systems", R.K. Melugin & H.-P. Röser, eds., pp.43-53; "*HAWC: A Far-Infrared Camera for SOFIA*"
3. Irwin, K.D. 1995, APL 66 (15), pp. 1998-2000, "*An application of electrothermal feedback for high resolution cryogenic particle detection*"
4. Welty, R.P. & Martinis, J.M. 1993, IEEE Trans. On Applied Superconductivity 3 (1), pp.2605-2608, "*Two-stage integrated SQUID amplifier with series array output*"

5. Chervenak, J.A., Irwin, K.D., Grossman, E.N., Martinis, J.M., Reintsema, C.D., & Huber, M.E. 1999 Applied Physics Letters, 74 (26), pp.4043-4045, "*Superconducting Multiplexer for Arrays of Transition Edge Sensors*"
6. Grossman, E.N. 1989, "AT-Atmospheric Transmission Software User's Manual, v1.5", Airhead Software Co., 2069 Bluff St., Boulder, CO 80302
7. Benford, D.J. et al. 1999, ASP Conference series #217, "Imaging at Radio through Submillimeter Wavelengths", p.134; "*Superconducting Bolometer Arrays for Submillimeter Astronomy*"
8. Staguhn, J.G. et al. 2001, AIP Conference proceedings #605, "Low Temperature Detectors", F.S. Porter et al., eds., pp.321-324, "*TES Detector Noise Limited Readout Using SQUID Multiplexers*"
9. Benford, D.J. et al. 2000, IJIMW 21 (12), pp.1909-1916; "*Multiplexed Readout of Superconducting Bolometers*"
10. Benford, D.J. et al. 2001, AIP Conference proceedings #605, "Low Temperature Detectors", F.S. Porter et al., eds., pp.589-592, "*First Astronomical Use of Multiplexed Transition Edge Bolometers*"
11. Irwin, K.D. et al. 2001, AIP Conference proceedings #605, "Low Temperature Detectors", F.S. Porter et al., eds., pp.301-304, "*Time-Division SQUID Multiplexers*"
12. Ames, T.J. & Case, L. 2002, these proceedings; "*Distributed Framework for Dynamic Telescope and Instrument Control*"
13. Voellmer, G.M. & Jackson, M.L. 2002, Proc. SPIE #4850, in press; "*Kinematic Kevlar Suspension System for the HAWC and SAFIRE ADR Salt Pills*"
14. Nikola, T., Hailey-Dunsheath, S., Stacey, G.J., Benford, D.J., & Moseley, S.H. 2002, Proc. SPIE #4855, in press; "*ZEUS: A Submillimeter Grating Spectrometer for Exploring Distant Galaxies*"